

# Hydrochemistry of Groundwater in the Rice Cultivation Area of Maga: Analysis of the Mineralization Process

Emmanuel Aguiza Abai<sup>1\*</sup>, Hugues Pahimi<sup>2</sup>, Prosper Samba Koukouare<sup>3</sup>,  
Guillaume Ewodo Mboudou<sup>4</sup>, Auguste Ombolo<sup>5</sup>

<sup>1</sup>Department of Industrial Security, Quality and Environment, National Advanced School of Mines and Petroleum Industries, University of Maroua, Kaele, Cameroon

<sup>2</sup>School of Chemical Engineering and Mineral Industries, University of Ngaoundere, Ngaoundere, Cameroon

<sup>3</sup>Department of Hydrocarbons Exploitation, Mao National Higher Petroleum Institute, N'Djamena, Chad

<sup>4</sup>Department of Hydraulics and Water Management, National Advanced School of Engineering of Maroua, University of Maroua, Maroua, Cameroon

<sup>5</sup>Department of Rural Engineering, Higher Institute of Agriculture, Forestry, Water and Environment, University of Ebolowa, Ebolowa, Cameroon

Email: \*aguiza\_abai@yahoo.fr

**How to cite this paper:** Abai, E. A., Pahimi, H., Koukouare, P. S., Mboudou, G. E., & Ombolo, A. (2024). Hydrochemistry of Groundwater in the Rice Cultivation Area of Maga: Analysis of the Mineralization Process. *Journal of Geoscience and Environment Protection*, 12, 370-387.

<https://doi.org/10.4236/gep.2024.129019>

**Received:** July 13, 2024

**Accepted:** August 20, 2024

**Published:** September 29, 2024

Copyright © 2024 by author(s) and Scientific Research Publishing Inc.

This work is licensed under the Creative Commons Attribution International License (CC BY 4.0).

<http://creativecommons.org/licenses/by/4.0/>



Open Access

## Abstract

The use of groundwater for drinking water supply to the population is increasingly practiced in the rice cultivation area of Maga. However, there is a lack of knowledge about the hydrochemical characteristics of this water due to a lack of quality control. This study aims to contribute to the understanding of mineralization processes in order to establish the hydrochemical profile of the water in the area. The methodological approach consisted of collecting fifteen water samples from wells and boreholes during six campaigns for physicochemical analysis, and studying them through methods of interpreting hydrochemical data. The analysis results show that these waters are moderately mineralized. The water facies are mainly of the bicarbonate sodium and potassium type, as well as the bicarbonate calcium and magnesium type. Calculation of saturation indices demonstrates that evaporite minerals show lower degrees of saturation than carbonate minerals, with gypsum, anhydrite, and halite being in a highly undersaturated state. The mineralization of groundwater originates from the dissolution of surrounding rocks on the one hand, and anthropogenic activities involving exchanges between alkalis ( $\text{Na}^+$  and  $\text{K}^+$ ) in the aquifer and alkaline earth ( $\text{Ca}^{2+}$  and  $\text{Mg}^{2+}$ ), resulting in the fixation of alkaline earth and the dissolution of alkalis.

---

## Keywords

Hydrochemistry, Mineralization, Groundwater, Maga

---

## 1. Introduction

Water is essential for life and holds great importance for countless human activities. Unfortunately, water resources are highly vulnerable to degradation and seriously threatened by human activities. Irrational use of fertilizers and pesticides in agricultural areas, coupled with a lack of environmental awareness among the population, leads to an imbalance in the ecosystem and generates pollutants that can affect the physicochemical quality of water. In addition to this anthropogenic phenomenon, natural mineralization occurs due to the dissolution of mineral elements contained in the rock over prolonged contact with water (Doumtoudjinodji et al., 2024; Compaore et al., 2020; Mulliss et al., 1997). In urban areas, the existence of good-quality drinking water supply networks allows the population to avoid diseases related to consuming contaminated water. However, rural populations sometimes have to rely on well and borehole water, or even surface water, for consumption (Dhin Etia et al., 2022; Djuissi Tekam et al., 2019; Nanfack et al., 2014; Wirmvem et al., 2013). However, relying on these different water resources of questionable quality exposes the population to health risks (Traoré et al., 2016).

The water supply for rice fields in the Maga area is done through gravity irrigation using water from an artificial lake. This lake is fed by the Mayos Tsanaga and Boula to the west, and by the Mayo Gerléo and the intake at Djafga on the Logone River to the southwest. The flow of water in a flat area carries clay and silt particles that reach aquatic environments through runoff along slopes or erosion of banks. These particles may carry adsorbed molecules that can be diffuse pollutants, which, through infiltration, can end up in the groundwater and thus alter water chemistry (Oumar et al., 2017; Nouzha et al., 2016; El Bliidi et al., 2006). However, the CBLT/BGR projects have highlighted the importance of numerous wetland areas in the Lake Chad Basin and their contribution to the renewal of groundwater resources in the basin, including the Maga rice fields (Seeber, 2013; Vassolo & Daïra, 2012). By examining research conducted in countries with high rice cultivation potential located in arid and semi-arid zones like Morocco (Laaouan et al., 2016; El Oumlouki et al., 2014; Amharref et al., 2007), Senegal (Sall & Vanclooster, 2009) and even Cameroon (Ahmadou et al., 2016), it has been shown that agricultural practices have an influence on the physicochemical quality of water in these areas.

The objective of this study is to contribute to the understanding of the hydrochemical characteristics of groundwater in the rice cultivation area of Maga and determine the processes responsible for the mineralization of groundwater in the area.

## 2. Materials and Methods

### 2.1. Study Area

The rice cultivation area of Maga is located in the Far North Region of Cameroon, in the Mayo-Danay department. This area covers an area of 2000 km<sup>2</sup> and is situated between 10°32'57" and 11°58'00" latitude North, and between 14°34' and 15°10'13" longitude East. The climate here is Sahelian-Sudanese, with a long dry season starting in early October and ending in early May, and a short rainy season from June to September characterized by heavy rainfall episodes. The rainfall varies between 530 and 630 mm/year, with peaks in August and September. The average temperature is 28°C, and the annual evapotranspiration is 1800 mm (Ngatcha et al., 2007). The morphological aspect is dominated by a floodplain that is part of an extensive geomorphological unit that extends to Nigeria, Niger, and Chad (Sighomnou, 2003).

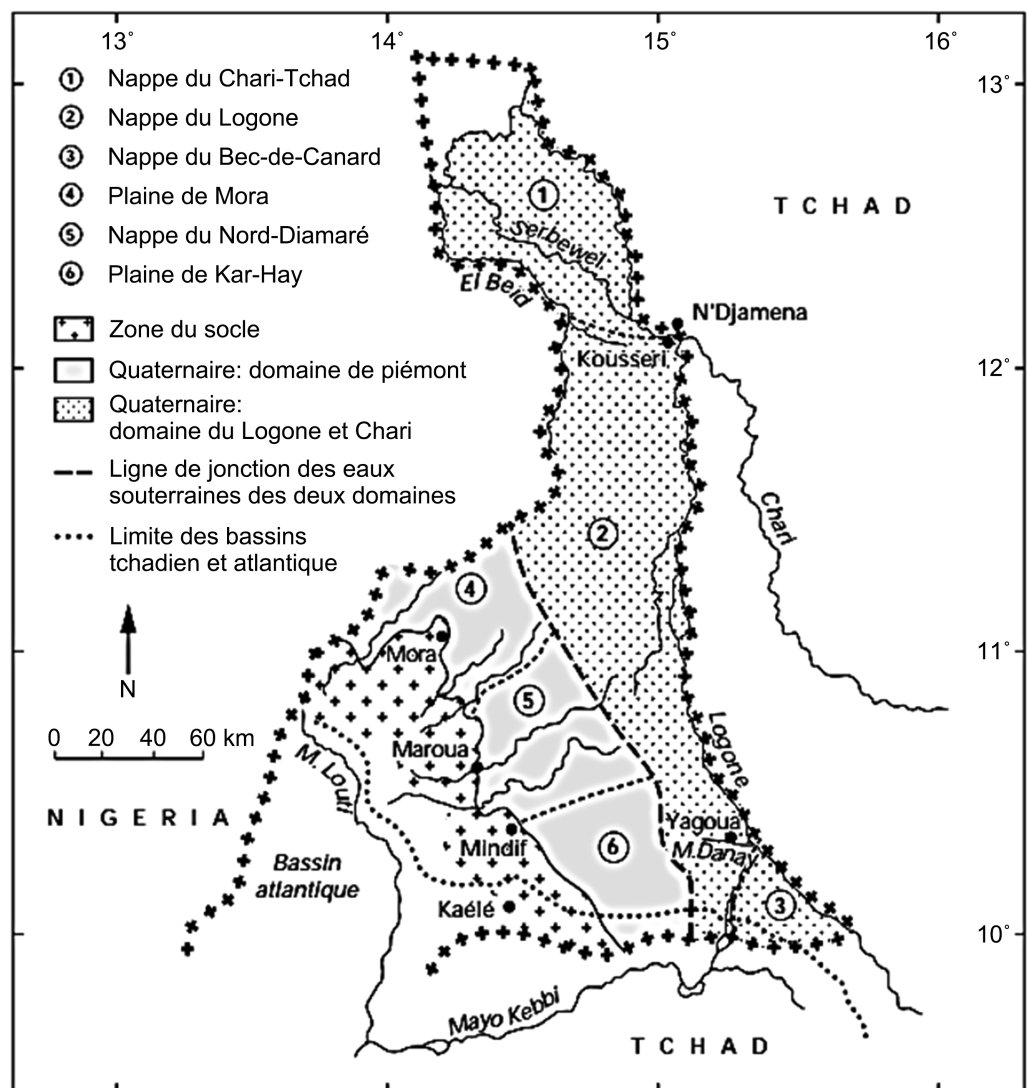


**Figure 1.** Hydrogeology of the Far North of Cameroon (modified after Detay, 1987).

## 2.2. Geological and Hydrogeological Framework

The study area (Maga) is located in the Logone-Chari floodplain, which consists of recent and old Quaternary formations from the Lake Chad Basin. The thickness of these formations generally varies between 50 and 70 m (Schneider & Wolff, 1992; Biscaldi, 1970). These sedimentary formations have a large extension and cover the central plain up to Lake Chad (Figure 1).

The Logone-Chari floodplain is composed of *yayrés*, which are territories prone to flooding by the Logone River and where water stagnated for five to seven months before the construction of the artificial lake and the SEMRY rice fields in Maga in 1979 (Ngatcha et al., 2007). In this area, the dominant soils are vertisols and hydromorphic black clays (Brabant & Gavaud, 1985). During the dry season, hydromorphic soils exhibit desiccation cracks that become waterlogged at the beginning of the rainy season. This waterlogging causes the soil to swell, the closure of these cracks, and a decrease in surface permeability. Previous studies on the analysis of the sources of water mineralization in the area by studying resistivity have shown a decrease in resistivity when moving from Logone to the west.

These studies have also highlighted some irregularities, such as the values of  $2000 \Omega\cdot\text{cm}^{-1}$  to  $3000 \Omega\cdot\text{cm}^{-1}$  in the southwest of Guirvidig, indicating a supply from surface waters. However, the low resistivities obtained between Pouss and Mazera indicate low infiltration of surface waters due to impermeable clayey soils (Seignobos & Moukouri, 2000). The majority of the waters belong to a calcareous carbonate facies, with a possible enrichment in sodium.

## 2.3. Sampling and Analytical Methods

In order to study the mineralization of groundwater, sampling was carried out during 06 campaigns from October 2017 to June 2019, resulting in a total of 90 samples. A network of 15 points was established to ensure good coverage of the variability of groundwater quality in the area. The selection of sampling points took into account parameters such as the depth of the groundwater level and the location of the point relative to the lithology. For all water samples, pH, temperature, TDS, and EC were measured in situ using a multiparameter probe (Hanna HI 98130). For chemical analysis, the samples were transported and stored in the laboratory according to standard methods of the WHO (2011). The main ions were analysed using the following methods: volumetry for calcium ( $\text{Ca}^{2+}$ ), magnesium ( $\text{Mg}^{2+}$ ), bicarbonates ( $\text{HCO}_3^-$ ) and chlorides ( $\text{Cl}^-$ ); spectrophotometry for sulfates ( $\text{SO}_4^{2-}$ ) and nitrates ( $\text{NO}_3^-$ ); flame photometry for sodium ( $\text{Na}^+$ ) and potassium ( $\text{K}^+$ ) ions. These analyses followed the recommended methods by Rodier (2009) and WHO (2011).

The obtained results of physicochemical analysis were processed using hydrochemical data interpretation methods. The Piper diagram (Piper, 1953) was used to determine the water typology, binary diagrams were used to understand the origin and processes of groundwater mineralization, and the Chadha diagram (Chadha, 1999) was used to identify various processes involved in groundwater

mineralization.

### 3. Results and Interpretation

#### 3.1. Hydro Chemical Characterization of Groundwater

The results of physicochemical analysis of groundwater during the observation period are recorded in **Table 1**.

The average (Aver) temperature of groundwater ranges between 29°C and 30°C. The lowest temperature recorded was 27°C in February 2019, while the highest was 34.1°C in February 2018. The pH values throughout the campaigns varied from 6.44 in October 2017 to 8.33 in October 2018. Generally, pH values near 8 were obtained in the Pouss area, while values closer to 6 were observed in the Guirvidig area. The spatial distribution of electrical conductivities varied on average between 110 µS/cm and 1260 µS/cm. The highest EC values were observed in October, which corresponds to the period of high-water levels in the study area.

The concentrations of Ca<sup>2+</sup> ranged from 0 to 61 mg/L. These extreme values were obtained during the same campaign in October 2017, which also had the highest average concentration (12 mg/L) and the highest standard deviation (19.63 mg/L) among all the campaigns. However, the concentration of Mg<sup>2+</sup> in the area varied from 3 to 28 mg/L over the six campaigns. The highest average concentration was observed in June 2019 with a value of 15.27 mg/L. The variation in concentrations during this campaign was remarkable, with the highest standard deviation (7.11) and a coefficient of variation of 0.47. Higher values were found in the Guirvidig area. Additionally, the concentrations of Na<sup>+</sup> throughout the campaigns ranged from 8 mg/L to 285 mg/L, with average concentrations ranging from 72.59 to 94.88 mg/L. The standard deviation and coefficient of variation were high, at 70.01 mg/L and 0.89, respectively. The lowest concentrations were observed during the dry season campaigns (February). The concentrations of K<sup>+</sup> were relatively low, with an average value ranging from 0.41 to 2.93 mg/L, a moderate standard deviation of 0.25, and a high coefficient of variation of approximately 1.54. The minimum and maximum values were 0.1 and 12.2 mg/L, respectively.

The concentrations of Cl<sup>-</sup> varied between 0 and 43 mg/L, with average concentrations ranging from 1.73 to 4.68 mg/L. The distribution of chloride concentrations was highly variable, as indicated by the standard deviation (ranging from 3.95 to 10.93) and coefficient of variation (ranging from 2.06 to 3.24). On the other hand, NO<sub>3</sub><sup>-</sup> concentrations ranged from 1 mg/L to 93.7 mg/L, with average concentrations ranging from 9.01 to 20.31 mg/L. The contribution of each sampling point to mineralization varied, as evidenced by standard deviations ranging from 7.0 to 21.35 and coefficients of variation ranging from 0.50 to 1.66 over the six campaigns. The values of SO<sub>4</sub><sup>2-</sup> ranged from 0 to 57 mg/L, with average concentrations ranging from 1.13 to 6.67 mg/L. The highest values were recorded during the October campaigns, which correspond to the high-water period, while the lowest concentrations were observed during the February campaigns, which represent the low-water period. Finally, the HCO<sub>3</sub><sup>-</sup> concentrations in groundwater ranged from 53

mg/L to 702.32 mg/L, with averages ranging from 233.30 to 355.90 mg/L. The concentrations varied considerably, with high standard deviations ranging from 120.72 to 171.33 and coefficients of variation ranging from 0.46 to 0.68.

**Table 1.** Variation of physicochemical parameters of groundwater.

Parameters	October-17					February-18					June-18				
	Min	Max	Aver	$\sigma$	CV	Min	Max	Aver	$\sigma$	CV	Min	Max	Aver	$\sigma$	CV
T°C	28.7	31.9	30.20	0.98	0.03	27.6	34.1	30.91	1.65	0.05	28.1	31.4	29.67	1.07	0.04
pH	6.44	8.16	7.25	0.56	0.08	6.7	8.3	7.47	0.46	0.06	6.8	8.24	7.48	0.43	0.06
EC	140	970	481.33	278.92	0.58	110	750	363.33	193.30	0.53	110	850	383.33	223.79	0.58
TDS (mg/L)	70	490	240.00	141.07	0.59	50	380	181.67	98.45	0.54	50	430	191.00	112.89	0.59
Ca <sup>2+</sup> (mg/L)	0	61	12.00	19.63	1.64	0	38	4.73	9.32	1.97	1	34	7.73	10.84	1.40
Mg <sup>2+</sup> (mg/L)	3	18	8.67	4.95	0.57	3	26	9.93	5.36	0.54	7	24	12.93	4.33	0.34
Na <sup>+</sup> (mg/L)	8.33	218.1	72.59	64.57	0.89	24.29	164.82	77.38	39.81	0.51	27.46	238.04	94.88	59.61	0.63
K <sup>+</sup> (mg/L)	2	12.2	2.93	2.58	0.88	1.9	5.8	2.38	0.97	0.41	2.1	2.8	2.39	0.25	0.11
Cl <sup>-</sup> (mg/L)	0	22	1.73	5.61	3.24	0.2	16.1	1.92	3.95	2.06	0	32	3.38	7.96	2.35
NO <sub>3</sub> <sup>-</sup> (mg/L)	1.8	75.9	10.99	18.28	1.66	3	31.3	9.01	7.40	0.82	2	36.6	12.13	9.68	0.80
SO <sub>4</sub> <sup>2-</sup> (mg/L)	1	57	6.67	15.67	2.35	0	4	1.13	0.99	0.87	0	9	1.47	2.17	1.48
HCO <sub>3</sub> <sup>-</sup> (mg/L)	53.64	546.56	253.48	171.33	0.68	101.28	702.32	300.64	168.57	0.56	136.64	694.96	355.9	164.42	0.46

Parameters	Oct-18					Févr-19									
	Min	Max	Aver	$\sigma$	CV	Min	Max	Aver	$\sigma$	CV	Min	Max	Aver	$\sigma$	CV
T°C	27.6	31.9	29.57	1.19	0.04	27	31.5	29.25	1.33	0.05	28.9	31.9	30.19	0.93	0.03
pH	6.62	8.33	7.30	0.47	0.06	6.69	8.01	7.31	0.40	0.05	6.8	7.99	7.37	0.38	0.05
CE	150	1260	408.00	297.47	0.73	110	850	378.00	230.01	0.61	110	780	379.33	221.92	0.59
TDS (mg/L)	80	630	205.33	148.03	0.72	50	420	190.67	114.80	0.60	50	390	188.00	109.95	0.58
Ca <sup>2+</sup> (mg/L)	0	13	2.40	3.04	1.27	1	14	2.67	3.29	1.23	1	56	9.20	15.00	1.63
Mg <sup>2+</sup> (mg/L)	3	14	8.47	3.23	0.38	3	23	10.47	5.30	0.51	8	28	15.27	7.11	0.47
Na <sup>+</sup> (mg/L)	23	285	88.60	70.51	0.80	15	186	78.43	50.78	0.65	12.7	201	74.98	52.61	0.70
K <sup>+</sup> (mg/L)	0.2	1	0.41	0.22	0.52	0.1	4	0.71	1.09	1.54	1.3	3.8	2.19	0.82	0.37
Cl <sup>-</sup> (mg/L)	0.3	43	4.68	10.93	2.34	0	32	2.77	8.12	2.94	0	20	1.69	5.08	3.01
NO <sub>3</sub> <sup>-</sup> (mg/L)	1	55.5	9.05	13.41	1.48	2.4	68.1	15.73	16.47	1.05	4.7	93.7	20.81	21.35	1.03
SO <sub>4</sub> <sup>2-</sup> (mg/L)	0	15	2.33	3.85	1.65	0	8	1.47	1.85	1.26	0	15	2.13	3.68	1.73
HCO <sub>3</sub> <sup>-</sup> (mg/L)	107.12	556.76	255.95	149.18	0.58	87.84	465.76	233.30	120.72	0.52	92.72	575.84	261.97	146.96	0.56

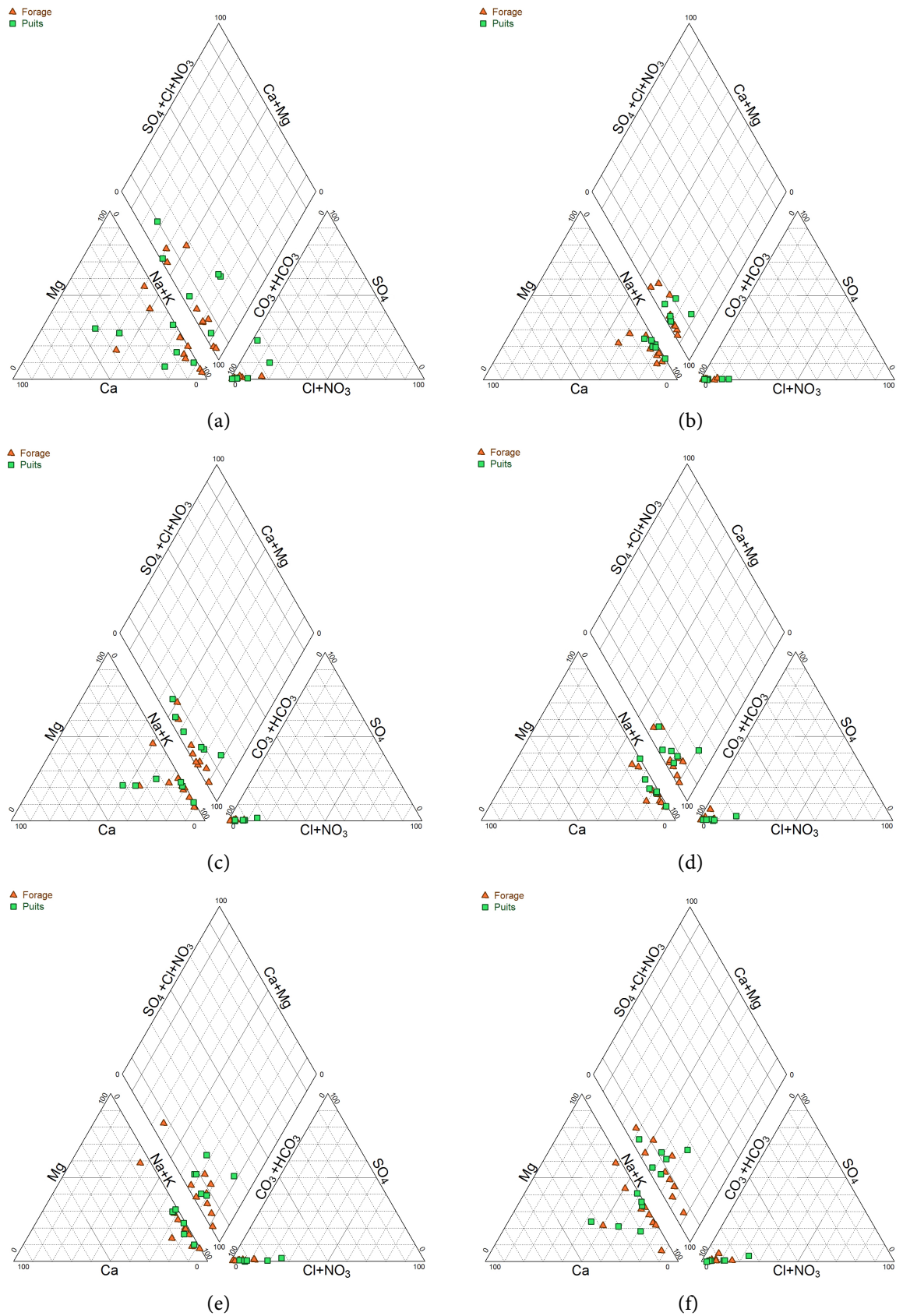


Figure 2. Piper diagram.

### 3.2. Identification of the Main Hydro Chemical Facies

The data on major ions plotted on the Piper diagram (Piper, 1953) generally show that the groundwater in the Maga irrigated rice perimeter is mainly of the bicarbonate-sodium and potassium, and bicarbonate-calcium and magnesium types (Figure 2). The first facies are characteristic of the waters of the cultivated areas of the irrigated perimeter of Maga East and West, and the second facies are dominant in the Pouss areas. The diagram indicates a dominance of weak acids for both water facies, with a dominance of alkaline earth metals in the bicarbonate-calcium and magnesium facies (Figure 2(a), Figure 2(c), Figure 2(e), Figure 2(f)), and a dominance of alkalis over alkaline earth metals in the bicarbonate-sodium and potassium facies (Figures 2(a)-(f)). Consequently, the waters in the cultivated area of the irrigated perimeter are enriched in sodium and potassium concerning cations, while bicarbonates remain the dominant anion.

The creation of a graphical representation of facies based on the quantities of reacting ions is important for confirming the presence of different facies characterizing groundwater. Given the dominance of bicarbonate, sodium, and magnesium ions, two diagrams (Figure 3) using the ratios  $\text{Na}^+/\text{Mg}^{2+} - \text{Cl}^-/\text{HCO}_3^-$  and  $\text{Na}^+/\text{Ca}^{2+} - \text{Cl}^-/\text{HCO}_3^-$  have been constructed. Both diagrams show the concentration of ion ratios in three poles with a predominance of the Bicarbonate Sodium facies, indicating the previously determined facies that characterize the aquifer. This result will lead to studying the source of mineralization by considering the overall average of all analyses.

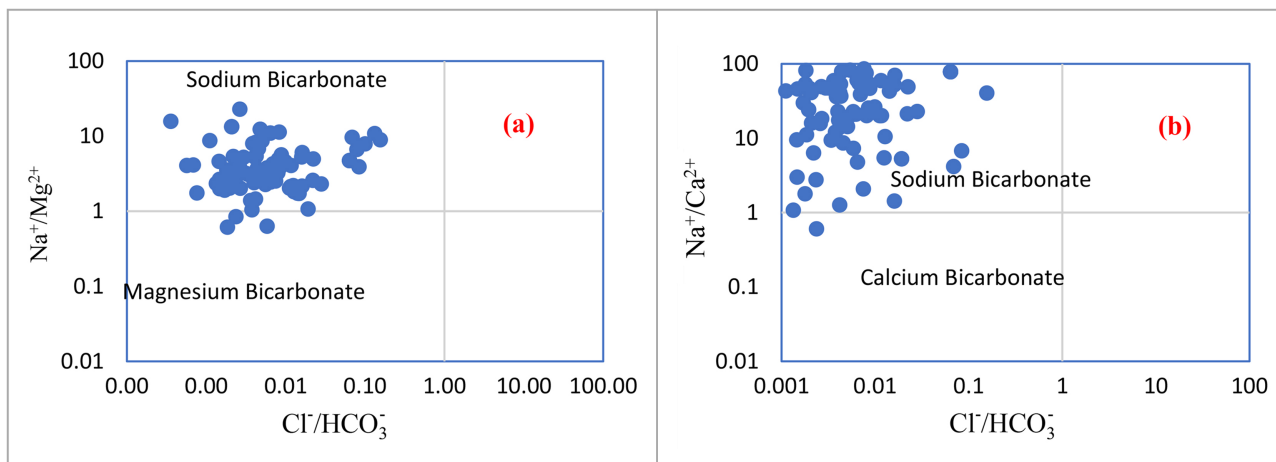


Figure 3. Distribution of chemical facies.

### 3.3. Study of the Origin of Water Chemistry and Mineralization of Groundwater

The dissolved chemical species in water and their relationships with each other can reveal the origin of mineralization and the processes that have contributed to the mineral composition of the analyzed water (Aboubaker et al., 2013; Diaw et al., 2012; Kuldip-Singh et al., 2011; Jalali, 2009; Gupta et al., 2008).

### 3.3.1. Saturation Indices of Mineral Phases

Saturation indices (SI) of minerals are used to evaluate mineralization because the water chemistry is controlled by the equilibrium of solid phases (Appelo & Postma, 1993). SI was calculated using PHREEQC V.2 (Parkhurst & Appelo, 1999), which can be accessed through the free version of the software Diagrammes (Simler, 2007). The software was utilized to calculate the SI of the following water minerals: calcite ( $\text{CaCO}_3$ ), dolomite  $\text{CaMg}(\text{CO}_3)_2$ , aragonite ( $\text{CaCO}_3$ ), anhydrite ( $\text{CaSO}_4$ ), gypsum ( $\text{CaSO}_4 \cdot 2\text{H}_2\text{O}$ ), and halite ( $\text{NaCl}$ ).

The calculations showed that carbonate minerals have different degrees of saturation. The saturation index of dolomite ranges from  $-3.31$  to  $-0.34$ , while the intervals for calcite vary from  $-2.19$  to  $-0.27$ , and aragonite SI ranges from  $-2.34$  to  $-0.41$  (Figure 4). Assuming equilibrium occurs within the range of  $-0.5$  to  $+0.5$ , the results indicate that dolomite, calcite, and aragonite are in an undersaturated state. Evaporite minerals exhibit lower degrees of saturation than carbonate minerals (Figure 4). Gypsum records indices ranging from  $-5.17$  to  $-3.11$ , followed by anhydrite with an index ranging from  $-5.39$  to  $-3.33$ , and finally halite with indices ranging from  $-9.64$  to  $-6.85$ . All these minerals are in a highly undersaturated state (Dindane et al., 2003).

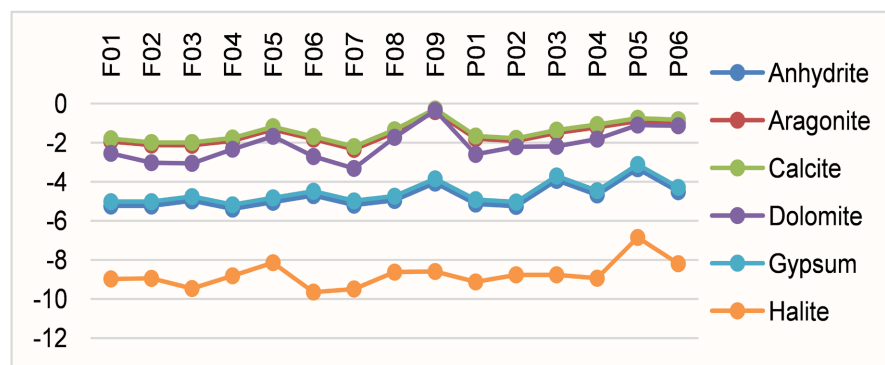
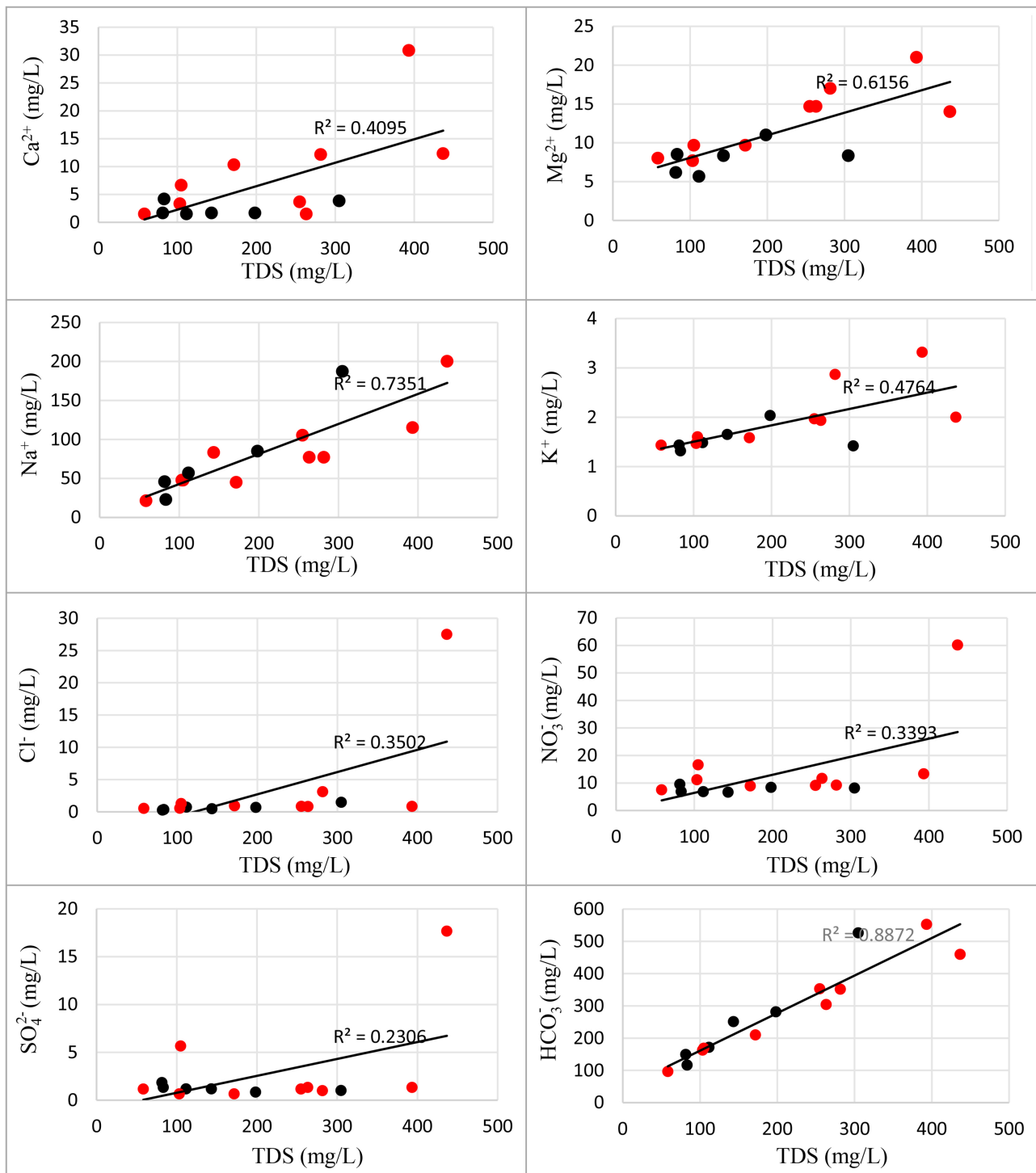


Figure 4. Variation of mineral saturation index.

### 3.3.2. Relationships between Total Mineralization and Major Ions

The study of correlations through binary graphs between the concentrations of major elements ( $\text{Ca}^{2+}$ ,  $\text{Mg}^{2+}$ ,  $\text{Na}^+$ ,  $\text{K}^+$ ,  $\text{Cl}^-$ ,  $\text{SO}_4^{2-}$ ,  $\text{HCO}_3^-$ , and  $\text{NO}_3^-$ ) and the total dissolved solids (TDS) (Figure 5) helps identify the origin of mineralization in the sampled water.

Observing Figure 5 highlights the contribution of each major element to the total mineralization of water. The results of chemical analysis of groundwater projected onto the binary diagrams have revealed a significant relationship between sodium and bicarbonates in water mineralization, with respective correlation coefficients of  $r = 0.73$  and  $r = 0.88$ . It also appears that magnesium ions ( $r = 0.61$ ) have a moderate influence on the mineral content of these groundwater samples. Calcium, potassium, chlorides, nitrates, and sulfates show only a weak relationship with mineralization ( $r = 0.40$ ,  $r = 0.47$ ,  $r = 0.35$ ,  $r = 0.33$ , and  $r = 0.23$ ).



**Figure 5.** Correlation of major chemical elements with total mineralization.

### 3.3.3. Binary Relationships between Major Elements

Dissolved chemical species and their relationships with each other can reveal the origin of solutes and the processes that have generated the chemical composition of water (Touhari, 2015). The interrelation is studied through the analysis of binary diagrams, which allow the identification of the source of dissolved salts in

water. Considering that the studied water facies are bicarbonate sodium to potassium, bicarbonate magnesium, and then calcic, diagrams  $\text{Na}^+ + \text{K}^+$  and  $\text{Ca}^{2+} + \text{Mg}^{2+}$  based on  $\text{HCO}_3^-$  appear most relevant.

### 1) $\text{Na}^+/\text{Cl}^-$ ratio

The  $\text{Cl}^-$  and  $\text{Na}^+$  ions present in groundwater can have various origins. Their presence can be natural, either linked to the dissolution of halite present in the surrounding geological formations, or due to inputs from meteoric precipitation, particularly enriched in  $\text{Cl}^-$  and  $\text{Na}^+$  from seawater. However, these ions can also have anthropogenic origins. The binary diagram (Figure 6(a)) representing the evolution of  $\text{Na}^+$  as a function of  $\text{Cl}^-$  shows an excess of  $\text{Na}^+$  content for almost all samples, indicating the existence of another source for sodium ions other than the dissolution of halite. The analytical data in Figure 6(a) deviating from the slope of 1 indicate that a significant fraction of sodium is associated with an anion other than chloride.

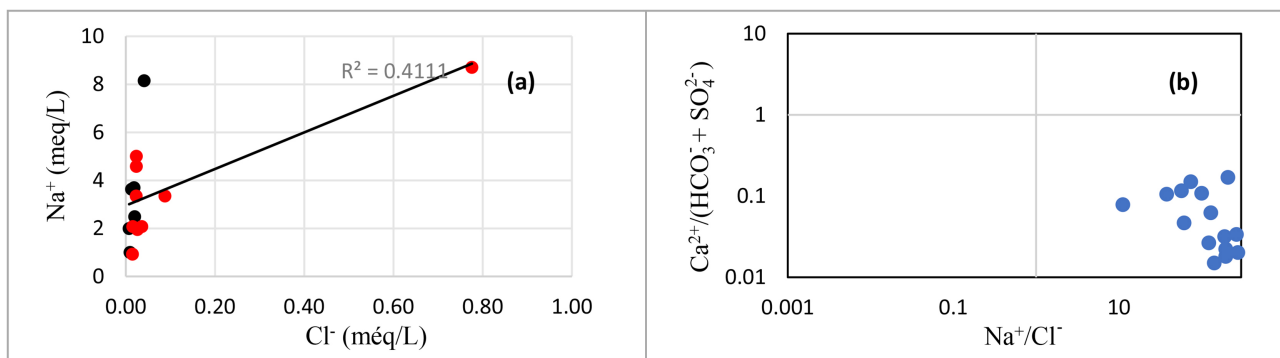
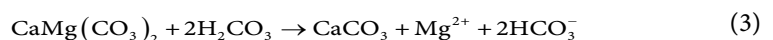
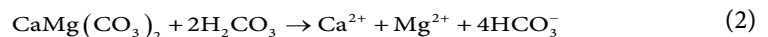


Figure 6. Determining the source of sodium.

### 2) $\text{Ca}^{2+}/\text{HCO}_3^-$ and $\text{Mg}^{2+}/\text{HCO}_3^-$ Ratio

The study of the relationship between the dissolved concentrations of  $\text{Ca}^{2+}$ ,  $\text{Mg}^{2+}$ , and  $\text{HCO}_3^-$  (Figure 7) in water allows for the identification of the main reactions involved in the dissolution of these ions, as described by the following equations [40]:



The linear correlation between  $\text{Ca}^{2+}$  and  $\text{HCO}_3^-$  allows for the classification of water points into two distinct groups. The first group, characterized by points located above the slope of 1, indicates an excess of  $\text{Ca}^{2+}$  compared to  $\text{HCO}_3^-$ , suggesting the dissolution of gypsum with an ion exchange effect. The second group consists of points below the slope of 1, indicating a deficit of  $\text{Ca}^{2+}$  compared to  $\text{HCO}_3^-$ . This could be explained by the secondary precipitation of calcite and dolomite and/or base exchange ( $\text{Na}^+$  for  $\text{Ca}^{2+}$  and  $\text{Mg}^{2+}$  for  $\text{Na}^+$ ) on the clay minerals of the aquifer, followed by carbonate dissolution.

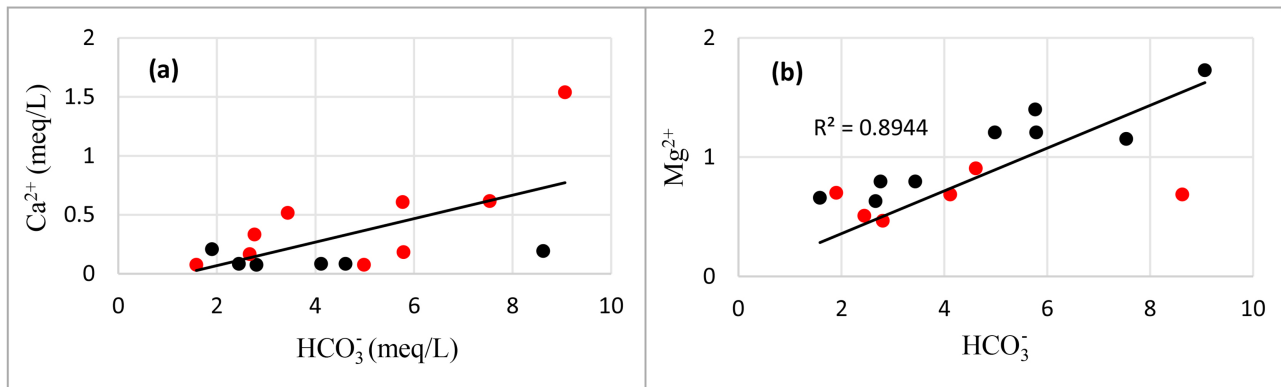


**Figure 7.** Distribution of water sampling points in relation to the dissolution line ((a): Calcite; (b): Dolomite).

### 3) $[(\text{Na}^+ + \text{K}^+) - \text{Cl}^-]$ vs $[(\text{Ca}^{2+} + \text{Mg}^{2+}) - (\text{SO}_4^{2-} + \text{HCO}_3^-)]$ ratio

To determine the dominant geochemical processes in groundwater, researchers have used various diagrams. One of these diagrams is the study of the relationship between  $[(\text{Na}^+ + \text{K}^+) - \text{Cl}^-]$  and  $[(\text{Ca}^{2+} + \text{Mg}^{2+}) - (\text{SO}_4^{2-} + \text{HCO}_3^-)]$ , which provides a clearer understanding of cation exchange processes by focusing solely on the reactions that may occur between clay minerals and the solution, while excluding ions potentially derived from other dissolution reactions of carbonate and evaporitic minerals (Farid et al., 2015; Kraiem et al., 2015; Garcia et al., 2001). Plotting the data obtained from water analyses on this diagram (Figure 8) shows that the samples are located in zones 3 and 4, where the difference between cations ( $\text{Ca}^{2+}$  and  $\text{Mg}^{2+}$ ) and anions ( $\text{HCO}_3^-$  and  $\text{SO}_4^{2-}$ ) is negative.

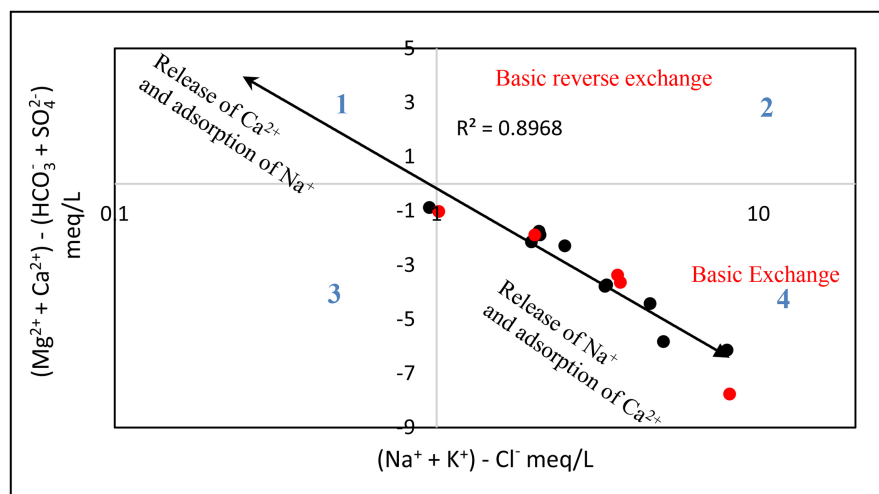


**Figure 8.** Correlation diagram between  $[(\text{Na}^+ + \text{K}^+) - \text{Cl}^-]$  vs  $[(\text{Ca}^{2+} + \text{Mg}^{2+}) - (\text{SO}_4^{2-} + \text{HCO}_3^-)]$ .

## 4. Discussion

The study of the physical parameters of water in the Maga rice-growing zone shows that the temperature varies little, with average values ranging from 29°C to

30°C throughout the seasons. This indicates a weak influence of ambient temperature on groundwater. The small variation in temperature also leads to a slight variation in pH, which remains within the standard range for drinking water (WHO, 2011).

The total mineralization of water, evaluated through measurements of electrical conductivity and total dissolved solids (TDS), indicates that the water is suitable for human consumption, with TDS values ranging from 50 to 630 mg/L on average (WHO, 2011). However, the values of electrical conductivity (EC), which range from 110  $\mu\text{S}/\text{cm}$  to 1260  $\mu\text{S}/\text{cm}$  on average, indicate that the groundwater is slightly to highly mineralized.

From a chemical perspective, ions play various roles in water mineralization. Calcium ions ( $\text{Ca}^{2+}$ ) are more concentrated in the western part of the area, following the direction of water flow. This indicates an accumulation of these ions due to both ion accumulation and the time of contact between water and rock. Magnesium ions ( $\text{Mg}^{2+}$ ) behave similarly to calcium ions, increasing in concentration along the direction of water flow. The high values of  $\text{Mg}^{2+}$  in the Guirvidig area can be explained by the quality of the soils, which consist of clay rich in montmorillonite, a clay family with a high content of  $\text{Mg}^{2+}$ ,  $\text{Ca}^{2+}$ , and  $\text{K}^+$  ions. Sodium ions ( $\text{Na}^+$ ) show a variable distribution from one point to another. The obtained standard deviation (70.01) and coefficient of variation (0.89) demonstrate the diverse sources of these ions in the water of the area. However, the overall trend of sodium concentrations follows the movement of groundwater. Sodium is present in the water through mineralization by contact with clay, where one  $\text{Ca}^{2+}$  ion is fixed after the release of two  $\text{Na}^+$  ions. The presence of  $\text{Na}^+$  in the water is usually associated with chloride pollution (Nouzha et al., 2016), as there is often a linear correlation between these two elements, as observed in this study. Indeed, the excess sodium in the study area, characterized by a ratio ( $\text{Na}/\text{Cl}$ ) > 1, is linked to the alteration of silicates, as shown by the work of Meybeck (1987) and Stallard and Edmond (1983). However, the increase in  $\text{Na}^+$  concentrations accompanying low  $\text{Cl}^-$  concentrations is due to the base exchange phenomenon, as the surrounding formations can release  $\text{Na}^+$  ions after fixing  $\text{Ca}^{2+}$ . The presence of potassium ions ( $\text{K}^+$ ) in the water is mainly the result of the alteration of potassium-rich clays and the dissolution of chemical fertilizers (NPK) extensively used in agriculture in the area.

Anions contribute to water mineralization to varying degrees. Chloride ions ( $\text{Cl}^-$ ) and nitrate ions ( $\text{NO}_3^-$ ) are moderately present, as well as sulfate ions ( $\text{SO}_4^{2-}$ ). Bicarbonate ions ( $\text{HCO}_3^-$ ) have a major contribution to the enrichment of ions in water. The high values of  $\text{HCO}_3^-$  depend on the presence of carbonate minerals in the soil and aquifer, the  $\text{CO}_2$  content in the air and soil in the catchment basin, as well as agricultural activities. The  $\text{HCO}_3^-$  concentrations in groundwater not influenced by anthropogenic factors typically range from 50 mg/L to 400 mg/L, with median values around 302 mg/L (Nouayti et al., 2015).

The analysis of Figure 5 reveals diverse correlations between chemical elements

and TDS, indicating various sources of mineralization that will be further corroborated by the study of saturation indices, which will show the equilibrium state between water and different minerals present in the solution (Yidana et al., 2008). Previous studies by Ngounou (1993) showed that bicarbonate ions ( $\text{HCO}_3^-$ ) had the predominant role in water mineralization among anions. They were mainly obtained in the aerated soil layers where silicate alteration reactions occur. On the other hand, sulfate ions ( $\text{SO}_4^{2-}$ ), chloride ions ( $\text{Cl}^-$ ), and nitrate ions ( $\text{NO}_3^-$ ) showed no dependency on bicarbonates, suggesting that their solubility is not linked to the process of alteration of aluminosilicate minerals but could come from meteoric and anthropogenic inputs. Regarding cations, calcium ions ( $\text{Ca}^{2+}$ ) were the main alkaline earth cations and were represented in surface-level waters. However, in deep waters, sodium ions ( $\text{Na}^+$ ) were the predominant alkali element. In summary, alkali-rich waters are more mineralized than waters dominated by alkaline earth elements.

However, the observations from the two binary diagrams (Figure 7(a) and Figure 7(b)) show that the ionic behavior is the same with the variation in calcium ( $\text{Ca}^{2+}$ ) and magnesium ( $\text{Mg}^{2+}$ ) concentrations, which are not correlated with bicarbonates ( $\text{HCO}_3^-$ ). This behavior indicates that the contribution of calcite and dolomite dissolution to water mineralization is weak and not the sole source of these elements. When examining the relationship between magnesium ions ( $\text{Mg}^{2+}$ ) and bicarbonates ( $\text{HCO}_3^-$ ), it is noticeable that most samples are located above the 1:1 line. This positioning above the 1:1 line may result from dolomitization, where magnesium ions are released into water while calcium ions are precipitated. The fact that the dolomitization process is more involved in water enrichment is also supported by the proximity of various samples to the 1:1 line.

The results from Figure 8 indicate that all groundwater samples in the aquifer system of the study area define a straight line ( $R^2 = 0.89$ ), indicating that the cations  $\text{Na}^+$ ,  $\text{Ca}^{2+}$ ,  $\text{Mg}^{2+}$ , and  $\text{K}^+$  participate in cation exchange reactions. This figure highlights base exchange interactions with clay minerals that affect the groundwater during surface water infiltration and their residence in the aquifer. In the absence of such reactions, all sample points should be located close to the origin point (McLean et al., 2000), which is not the case here. The samples situated in zones 3 and 4, with a negative difference between cations ( $\text{Ca}^{2+}$  and  $\text{Mg}^{2+}$ ) and anions ( $\text{HCO}_3^-$  and  $\text{SO}_4^{2-}$ ), indicate that the base exchange process dominates, as shown in Figure 6(b). In these zones (3 and 4), there is a release of alkaline ions ( $\text{Na}^+$  and  $\text{K}^+$ ) and the retention of alkaline earth elements ( $\text{Ca}^{2+}$  and  $\text{Mg}^{2+}$ ) in the clays.

## 5. Conclusion

The results of the physicochemical analysis of the water show that these waters are moderately mineralized with variable electrical conductivity (EC) values. On average, these values range from 110  $\mu\text{S}/\text{cm}$  to 1260  $\mu\text{S}/\text{cm}$ . The pH of the water in Maga is slightly neutral overall, indicating that the alkalinity is mainly controlled

by bicarbonates. The classification of water types using the Piper diagram shows that, almost all samples are of the sodium and potassium bicarbonate type, as well as the calcium and magnesium bicarbonate type. The calculation of water saturation indices shows that carbonate minerals have varying degrees of saturation, with dolomite, calcite, and aragonite being under saturated. However, evaporite minerals show lower degrees of saturation compared to carbonate minerals. Gypsum, anhydrite, and halite are highly undersaturated. The alteration of silicate minerals combined with base exchange processes allows for an understanding of the mineralization acquisition processes in groundwater, resulting from the dissolution of surrounding rocks, as well as anthropogenic activities. There is an exchange between the alkalis ( $\text{Na}^+$  and  $\text{K}^+$ ) in the aquifer and the alkaline earth elements ( $\text{Ca}^{2+}$  and  $\text{Mg}^{2+}$ ), leading to the fixation of alkaline earth elements and the solubilisation of alkalis. These processes can be illustrated by projecting the groundwater points onto the Chadha diagram. However, an isotopic study of the waters in the area is necessary in order to highlight the presence of chemical elements resulting from fertilization in the waters for a better understanding of the mineralization process.

### Conflicts of Interest

The authors declare no conflicts of interest regarding the publication of this paper.

### References

- Aboubaker, M., Jalludin, M., & Razack, M. (2013). Hydrochemistry of a Complex Volcano-Sedimentary Aquifer Using Major Ions and Environmental Isotopes Data: Dalha Basalts Aquifer, Southwest of Republic of Djibouti. *Environmental Earth Sciences*, *70*, 3335-3349. <https://doi.org/10.1007/s12665-013-2398-8>
- Ahmadou, Y., Kouebou, C., Malaa, D., Bourou, S., Olina, J. P., & Mbiandoun, M. (2016). Les engrais et les pesticides dans la riziculture périurbaine de la ville de Ga-roua, au Nord-Cameroun: Cas de Nassarao et Boklé. *International Journal of Innovation and Applied Studies*, *18*, 26-35.
- Amharref, M., Aassine, S., Bernoussi, A. S., & Haddouchi, B. Y. (2007). Cartographie de la vulnérabilité à la pollution des eaux souterraines: Application à la plaine du Gharb (Maroc). *Revue des sciences de l'eau*, *20*, 185-199. <https://doi.org/10.7202/015812ar>
- Appelo, C. A. J., & Postma, D. (1993). *Geochemistry, Groundwater & Pollution* (1st ed.). A. A. Balkema Publishers, 536 p.
- Biscaldi, R. (1970). *Carte Hydrogéologique de la plaine du Tchad Eaux souterraines Echelle: 1/200000 Notice Explicative*. BRGM.
- Brabant, P., & Gavaud, M. (1985). *Soils and Land Resources in Northern Cameroon. Coll Notice Explicative 103*. MESIRES-IRA Yaounde, ORSTOM, 285 p.
- Chadha, D. K. (1999). A Proposed New Diagram for Geochemical Classification of Natural Waters and Interpretation of Chemical Data. *Hydrogeology Journal*, *7*, 431-439. <https://doi.org/10.1007/s100400050216>
- Compaore, H., Ilboudo, S., Bambara, D., & Bama Nati, A. D. (2020). Pratiques paysannes d'utilisation des pesticides et pollution environnementale dans la commune de dano, province du ioba Burkina Faso. *Asian Journal of Science and Technology*, *11*, 10602-

10610.

- Detay, M. (1987). *Prospection et identification des aquifères: Reconnaissances préliminaires et méthode d'implantation des ouvrages par étude de terrain et photo-interprétation*. Session internationale de formation au Cefigre: Exploitation et gestion des ressources en eau souterraine.
- Dhin Etia, F. C., Mvogo, G., & Honoré, B. (2022). Les déterminants d'accès à l'eau potable au Cameroun. *African Development Review*, *34*, 154-170.  
<https://doi.org/10.1111/1467-8268.12624>
- Diaw, M., Faye, S., Stichler, W., & Maloszewski, P. (2012). Isotopic and Geochemical Characteristics of Groundwater in the Senegal River Delta Aquifer: Implication of Recharge and Flow Regime. *Environmental Earth Sciences*, *66*, 1011-1020.  
<https://doi.org/10.1007/s12665-010-0710-4>
- Dindane, K., Bouchaou, L., Hsissou, Y., & Krimissa, M. (2003). Hydrochemical and Isotopic Characteristics of Groundwater in the Souss Upstream Basin, Southwestern Morocco. *Journal of African Earth Sciences*, *36*, 315-327.  
[https://doi.org/10.1016/s0899-5362\(03\)00050-2](https://doi.org/10.1016/s0899-5362(03)00050-2)
- Djuissi Tekam, D., Vogue, N., Nkfusai, C. N., Ebode Ela, M., & Cumber, S. N. (2019). Accès à l'eau potable et à l'assainissement: Cas de la commune d'arrondissement de Douala V (Cameroun). *Pan African Medical Journal*, *33*, Article 33.  
<https://doi.org/10.11604/pamj.2019.33.244.17974>
- Doumtoudjinodji, P., Bernadin, E. M., Mbaigane, J. C. D., Djoueingue, N., Agnichola, U., & Amadou, A. S. (2024). Hydrochemical Characterisation and Assessment of the Level of Contamination of Groundwater Collected by Private Waterworks in the Town of Moundou in the South of Chad. *Journal of Geoscience and Environment Protection*, *12*, 13-32. <https://doi.org/10.4236/gep.2024.121002>
- El Blidi, S., Fekhaoui, M., Serghini, A., & Abidi, A. (2006). Rizières de la plaine du Gharb (Maroc): Qualité des eaux superficielles et profondes. *Bulletin de l'Institut Scientifique, Section Sciences de la Vie*, *28*, 55-60.
- El Oumlouki, K., Moussadek, R., Zouahri, A., Dakak, H., Chati, M., & El amrani, M. (2014). Étude de la qualité physico-chimique des eaux et des sols de la région Souss Massa, (Cas de périmètre Issen), Maroc. *Journal of Materials and Environmental Science*, *5*, 2365-2374.
- Farid, I., Zouari, K., Rigane, A., & Beji, R. (2015). Origin of the Groundwater Salinity and Geochemical Processes in Detrital and Carbonate Aquifers: Case of Chougafiya Basin (central Tunisia). *Journal of Hydrology*, *530*, 508-532.  
<https://doi.org/10.1016/j.jhydrol.2015.10.009>
- Garcia, G., del V. Hidalgo, M., & Blesa, M. (2001). Geochemistry of Groundwater in the Alluvial Plain of Tucumán Province, Argentina. *Hydrogeology Journal*, *9*, 597-610.  
<https://doi.org/10.1007/s10040-001-0166-4>
- Gupta, S., Mahato, A., Roy, P., Datta, J. K., & Saha, R. N. (2008). Geochemistry of Groundwater, Burdwan District, West Bengal, India. *Environmental Geology*, *53*, 1271-1282.  
<https://doi.org/10.1007/s00254-007-0725-7>
- Jalali, M. (2009). Geochemistry Characterization of Groundwater in an Agricultural Area of Razan, Hamadan, Iran. *Environmental Geology*, *56*, 1479-1488.  
<https://doi.org/10.1007/s00254-008-1245-9>
- Kraiem, Z., Zouari, K., Bencheikh, N., Agoun, A., & Abidi, B. (2015). Processus de minéralisation de la nappe du Plio-Quaternaire dans la plaine de Segui-Zograta (Sud-Ouest Tunisien). *Hydrological Sciences Journal*, *60*, 534-548.

- <https://doi.org/10.1080/02626667.2013.877587>
- Kuldip-Singh, Hundal, H. S., & Dhanwinder-Singh, (2011). Geochemistry and Assessment of Hydrogeochemical Processes in Groundwater in the Southern Part of Bathinda District of Punjab, Northwest India. *Environmental Earth Sciences*, *64*, 1823-1833. <https://doi.org/10.1007/s12665-011-0989-9>
- Laaouan, M., Aboulhassan, M.A., Bengamra, S., Taleb, A., Souabi, S., Tahiri, M. (2016). Comparative study of three groundwater pollution cities of Mohammedia, Temara and Dar Bouazza by nitrates (Moroccan Meseta). *Journal of Materials and Environmental Science*, *7*, 1298-1309.
- McClean, W., Jankowski, J., & Lavitt, N. (2000). Groundwater Quality and Sustainability in an Alluvial Aquifer, Australia. In O. Sililo et al. (Eds.), *Groundwater, Past Achievement and Future Challenges* (pp. 567-573). A. A. Balkema.
- Meybeck, M. (1987). Global Chemical Weathering of Surficial Rocks Estimated from River Dissolved Loads. *American Journal of Science*, *287*, 401-428. <https://doi.org/10.2475/ajs.287.5.401>
- Mulliss, R., Revitt, D. M., & Shutes, R. B. E. (1997). The Impacts of Discharges from Two Combined Sewer Overflows on the Water Quality of an Urban Watercourse. *Water Science and Technology*, *36*, 195-199. <https://doi.org/10.2166/wst.1997.0665>
- Nanfack, N. A. C., Fonteh, F. A., Payne, V. K., Katte, B., & Fogoh, J. M. (2014). Eaux non conventionnelles: Un risque ou une solution aux problèmes d'eau pour les classes pauvres. *Larhyss Journal*, *17*, 47-64.
- Ngatcha, B. N., Mudry, J., Aranyossy, J. F., Naah, E., & Reynault, J. S. (2007). Apport de la géologie, de l'hydrogéologie et des isotopes de l'environnement à la connaissance des «nappes en creux» du Grand Yaéré (Nord Cameroun). *Revue des sciences de l'eau*, *20*, 29-43. <https://doi.org/10.7202/014905ar>
- Ngounou, N. B. (1993). *Hydrogéologie des aquifères complexes en zone semi-aride-Les aquifères quaternaires des Grandes Yaérés (Nord Cameroun)* (357 p). Thèse du Doctorat. Université Joseph Fourir - Grenoble I.
- Nouayti, N., Khattach, D., & Hilali, M. (2015). Evaluation de la qualité physico-chimique des eaux souterraines des nappes du Jurassiques du haut bassin de Ziz (haut Atlas central, Maroc). *Journal of Materials and Environmental Science*, *6*, 1068-1081.
- Nouzha, B., Kacem, S. A., Ferdaouss, L., Aberrahim, L., & Mohammed, B. (2016). Evaluation De L'impact De La Pollution Agricole Sur La Qualité Des Eaux Souterraines De La Nappe Du Gharb. *European Scientific Journal*, *12*, 509. <https://doi.org/10.19044/esj.2016.v12n11p509>
- Oumar, F., Ahoussi, K. E., & Koffi, A. S. (2017). Cartographie Et Identification Des Activités Sources De Nuisances Et De Pollutions Dans Le Bassin Versant Du Barrage Du Kan De Bouake (Côte d'Ivoire). *European Scientific Journal*, *13*, 303. <https://doi.org/10.19044/esj.2017.v13n5p303>
- Parkhurst, D. L., & Appelo, C. A. J. (1999). *User's Guide to PHREEQC (Version 2)—A Computer Program for Speciation, Batch-Reaction, One-Dimensional Transport, and Inverse Geochemical Calculations*. United States Geological Survey, Water Resources Investigations Report 99-4259, 326 p.
- Piper, A. M. (1953). *A Graphic Procedure in the Geochemical Interpretation of Water Analyses* (p. 14). Ground Water Notes No. 12, USGS.
- Rodier, J. (2009). *L'analyse de l'eau* (9ème éd., 1526 p). Dunod.
- Sall, M., & Vanclooster, M. (2009). Assessing the Well Water Pollution Problem by Nitrates in the Small Scale Farming Systems of the Niayes Region, Senegal. *Agricultural Water*

- Management*, 96, 1360-1368. <https://doi.org/10.1016/j.agwat.2009.04.010>
- Schneider, J. L., & Wolff, J. P. (1992). *Carte Géologique et Carte Hydrogéologique 1/1500000 de la république du Tchad Mémoire Explicatif Vol. 1*. BRGM. N°209.
- Seeber, K. (2013). *2nd Discharge Measurements at Chari, Logone and Koulambou River, Chad Report N°6*. BGR-CBLT.
- Seignobos, C., & Moukouri, H. K. (2000). *Potentialités des sols et terroirs agricoles: Atlas de la Province de l'Extrême-Nord Cameroun* (p. 3). Atlas de la Province de l'Extrême-Nord is the publisher support.
- Sighomnou, D. (2003). *Gestion intégrée des eaux de crues—Cas de la plaine d'inondation du fleuve Logone*. WMO-GWP, 18 p.
- Simler, R. (2007). *Diagramme "Logiciel Libre du Laboratoire d'Hydrogéologie"*. Univ. Avignon (France).
- Stallard, R. F., & Edmond, J. M. (1983). Geochemistry of the Amazon: 2. The Influence of Geology and Weathering Environment on the Dissolved Load. *Journal of Geophysical Research: Oceans*, 88, 9671-9688. <https://doi.org/10.1029/jc088ic14p09671>
- Touhari, F. (2015). *Etude de la Qualité des Eaux de la vallée du Haut Cheliff*. Thèse de Doctorat, Ecole Nationale Supérieure d'Hydraulique, 179 p.
- Traoré, A., Mulaudzi, K., Chari, G., Foord, S., Mudau, L., Barnard, T. et al. (2016). The Impact of Human Activities on Microbial Quality of Rivers in the Vhembe District, South Africa. *International Journal of Environmental Research and Public Health*, 13, Article 817. <https://doi.org/10.3390/ijerph13080817>
- Vassolo, S., & Daira, D. (2012). *Project Activities—Report N°4*. HBGRCLT, 2012. <http://www.bgr.bund.de/lcbc>
- WHO (2011). *Guidelines to Drinking-Water Quality* (4th ed., p. 564). NLM Classification: WA 675. OMS.
- Wirmvem, M. J., Fantong, W. Y., Wotany, E. R., Takeshi, O., & Ayonghe, S. N. (2013). Sources of Bacteriological Contamination of Shallow Groundwater and Health Effects in Ndop Plain, Northwest Cameroon. *Journal of Environmental Science and Water Resources*, 2, 127-132.
- Yidana, S. M., Ophori, D., & Banoeng-Yakubo, B. (2008). A Multivariate Statistical Analysis of Surface Water Chemistry Data—The Ankobra Basin, Ghana. *Journal of Environmental Management*, 86, 80-87. <https://doi.org/10.1016/j.jenvman.2006.11.023>